CHIN. PHYS. LETT. Vol. 28, No. 1 (2011) 018701

Frequency-Locking in a Spatially Extended Predator-Prey Model

YU Cun-Juan(尉存娟)**, TAN Ying-Xin(谭迎新)

School of Chemical Engineering and Environmental, North University of China, Taiyuan 030051

(Received 3 September 2010)

The study is concerned with the effect of variable dispersal rates on Turing instability of a spatial Holling–Tanner system. A series of numerical simulations show that the oscillatory Turing pattern can emerge due to period diffusion coefficient. Moreover, we find that when the amplitude is above a threshold, 1 : 1 frequency-locking oscillation can be obtained. The results show that period diffusion coefficient plays an important role on the pattern formation in the predator-prey system.

PACS: 87. 23. Cc, 82. 40. Ck, 05. 45. Pq DOI: 10.1088/0256-307X/28/1/018701

Since the classical Lotka–Volterra models have some limitations to describe many realistic phenomena in biology, in some cases, they should make way to more sophisticated models from both a mathematical and biological point of view. In order to describe well the real ecological interactions between the species such as mite and spider mite, lynx and hare, sparrow and sparrow hawk, etc. by Tanner,[1] Wollkind *et al.*,[2] May developed a model, also known as the Holling–Tanner prey-predator model[3] in which he incorporated Holling's rate.[4–8] We first pay attention to the following Holling–Tanner model:

$$\frac{dx}{d\tau} = rx\Big(1 - \frac{x}{K}\Big) - \frac{mxy}{x + C}, \tag{1a}$$

$$\frac{dy}{d\tau} = y\Big[\theta\Big(1 - \frac{hy}{x}\Big)\Big], \tag{1b}$$

where x and y denote, respectively, the prey and predator populations. The first equation states that in the absence of predation the prey grow logistically with carrying capacity K and intrinsic growth rate r. The saturating predator functional response $mx/(C+x)$ used in Eq. (1) is of the Michaelis–Menten type in enzyme-substrate kinetics. The parameter m is the maximum specific rate of product formation, and C (the half-saturation constant) is the substrate density at which the rate of product formation is half the maximum. The second equation shows that predators grow logistically with intrinsic growth rate θ and carrying capacity proportional to the prey populations size x. The parameter h is the number of prey required to support one predator at equilibrium when y equals to x/h.

By taking

$$u = \frac{x}{K}, \quad v = \frac{my}{rK}, \quad t = r\tau, \tag{2a}$$

$$\delta = \frac{C}{K}, \quad \eta = \frac{\theta}{r}, \quad \gamma = \frac{hr}{m}, \tag{2b}$$

we arrive at the following equations containing dimensionless quantities:

$$\frac{du}{dt} = u(1-u) - \frac{uv}{u+\delta}, \tag{3a}$$

$$\frac{dv}{dt} = v\Big[\eta\Big(1 - \frac{\gamma v}{u}\Big)\Big]. \tag{3b}$$

Previous works focused on the stability analysis of the model.[1,2] However, the investigations have revealed that spatial inhomogeneities like the inhomogeneous distribution of nutrients as well as interactions on spatial scales, which are essentially based on the assumption that the motion of individuals of given population is random, can have an important impact on the dynamics of ecological populations.[9–11]

On the other hand, there has been some work only on the diffusion model with constant diffusion coefficients in the Holling–Tanner model and obtained stationary patterns.[6,12–15] However, the influence of period diffusion coefficient in predator-prey models, especially on the pattern formation of the populations, has received surprisingly little attention in the literature. In the present analysis, we are intended to study this effect. As a result, the following reaction-diffusion system is obtained as a model for predator-prey trophic interaction with period diffusion coefficient:

$$\frac{\partial u}{\partial t} = f(u,v) + d_1\nabla^2 u, \tag{4a}$$

$$\frac{\partial v}{\partial t} = g(u,v) + d_2(1 + A\cos(2B\pi t))\nabla^2 v, \tag{4b}$$

with

$$f(u,v) = u(1-u) - \frac{uv}{u+\delta}, \tag{5}$$

$$g(u,v) = v\Big[\eta\Big(1 - \frac{\gamma v}{u}\Big)\Big], \tag{6}$$

where $\nabla^2 = \partial^2/\partial x^2 + \partial^2/\partial y^2$ is the usual Laplacian operator in two-dimensional space and d_1, d_2 are, respectively, prey and predator diffusion coefficients. Here A and B are the controlled parameters.

First, we are interested in studying the stability behavior of the interior (positive) equilibrium point $E^* = (u^*, v^*)$, where

$$u^* = \gamma v^*, \tag{7a}$$

**Email: cunjuanyu@yahoo.cn

© 2011 Chinese Physical Society and IOP Publishing Ltd

$$v^* = \frac{\gamma - 1 - \gamma\delta + \sqrt{(\gamma - 1 - \gamma\delta)^2 + 4\delta\gamma^2}}{2\gamma^2}, \quad (7b)$$

obviously from biological reason with $A = 0$. We address the temporal stability of the uniform states which is associated with non-uniform perturbations[16–20]

$$\begin{pmatrix} u \\ v \end{pmatrix} = \begin{pmatrix} u^* \\ v^* \end{pmatrix} + \varepsilon \begin{pmatrix} u_\kappa \\ v_\kappa \end{pmatrix} e^{\lambda t + i\kappa x} + \text{c.c.} + \mathcal{O}(\varepsilon^2), \quad (8)$$

where λ is the perturbation growth rate, κ is the wavenumber (in the Turing domain, the system are stable with respect to homogeneous perturbations but lose their stability with respect to perturbations of specific wavenumbers κ), and c.c. stands for complex conjugate. The linear instability ($\varepsilon \ll 1$) of each one of the uniform states, is deduced from the dispersion relations. Substituting expression (8) into Eq. (4) and neglecting all nonlinear terms in u and v, one finds the characteristic equation for the growth rate λ as determinant of J,

$$\mathrm{J} = \begin{pmatrix} \lambda - a_{11} + d_1\kappa^2 & -a_{12} \\ -a_{21} & \lambda - a_{22} + d_2\kappa^2 \end{pmatrix}, \quad (9)$$

where $a_{11} = \partial f/\partial u$, $a_{12} = \partial f/\partial v$, $a_{21} = \partial g/\partial u$, and $a_{22} = \partial g/\partial v$ are the partial derivatives evaluated at the steady state E^*.

We obtain that the eigenvalue is the root of the following equation:

$$\lambda^2 + A_\kappa\lambda + B_\kappa = 0, \quad (10)$$

where

$$A_\kappa = (d_1 + d_2)\kappa^2 - (a_{11} + a_{22}), \quad (11a)$$

$$B_\kappa = d_1 d_2 \kappa^4 - (d_2 a_{11} + d_1 a_{22})\kappa^2 + a_{11}a_{22} - a_{12}a_{21}. \quad (11b)$$

Therefore, the solution to Eq. (10) is given by

$$\lambda_\kappa = \frac{-A_\kappa \pm \sqrt{A_\kappa^2 - 4B_\kappa}}{2}. \quad (12)$$

In the bifurcation point, two equilibrium states of the model intersect and exchange their stability. Biologically speaking, this bifurcation corresponds to a smooth transition between equilibrium states. To the Hopf bifurcation, it is space-independent and breaks the temporal symmetry of a system, which gives rise to oscillations that are uniform in space and periodic in time. The Turing bifurcation breaks spatial symmetry, leading to the formation of patterns that are stationary in time and oscillatory in space.

Mathematically speaking, the Hopf bifurcation occurs when

$$\mathrm{Im}(\lambda_\kappa) \neq 0, \quad \mathrm{Re}(\lambda_\kappa) = 0 \quad \text{at} \quad \kappa = 0, \quad (13)$$

and the Turing bifurcation occurs when

$$\mathrm{Im}(\lambda_\kappa) = 0, \quad \mathrm{Re}(\lambda_\kappa) = 0 \quad \text{at} \quad \kappa = \kappa_T. \quad (14)$$

Figure 1(a) shows the stability diagram of the spatially uniform steady state (SS) of the autonomous system in the (η, d_2) plane. The Hopf bifurcation line (Hopf) is horizontal at $\eta = 0.3238033021$. It crosses the Turing bifurcation line (Turing) at $d_2 = 6.16$. Figure 1(b) shows the dispersion curves at the designated points in Fig. 1(a).

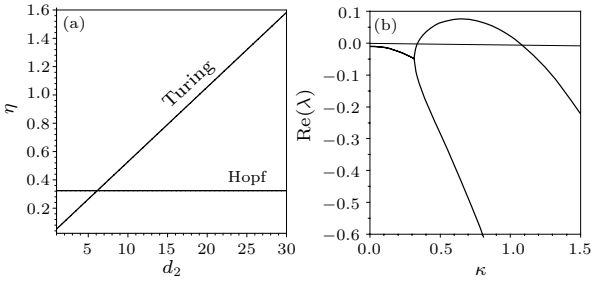

Fig. 1. Stability analysis of the Holling–Tanner model with $A = 0$. (a) Bifurcation diagram, $\eta_H = 0.3238033021$ and $\eta_T = 0.0527681795 d_2$, with fixed $\delta = 0.01$, $\gamma = 13/9$ and $d_1 = 1$. (b) Dispersion relations showing stable Hopf mode and unstable Turing mode corresponding to the point a in Fig. 1(a).

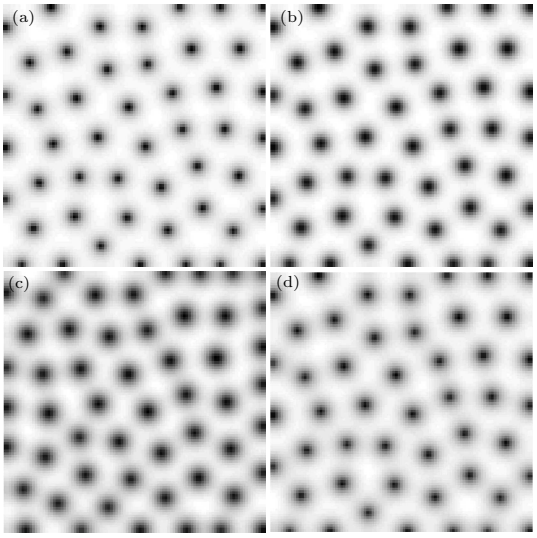

Fig. 2. Snapshots of contour pictures of the time evolution of the prey in a period with $\delta = 0.01$, $\gamma = 13/9$, $d_1 = 1$, $d_2 = 25$, $\eta = 0.52$, and $A = B = 1$: (a) $t = 100$; (b) $t = 120$; (c) $t = 140$; (d) $t = 160$. Here the period is $T = 60$. Black means high density and white low density.

All our simulations employ periodic boundary conditions with a system size of 100×100 space units. The spacing between the lattice points is defined by the lattice constant Δh. In the discrete system the Laplacian describing diffusion is calculated using finite differences, i.e., the derivatives are approximated by differences over Δh. For $\Delta h \to 0$ the differences approach the derivatives. The time evolution is also discrete, i.e., the time goes in steps of Δt. The time evolution can be solved by using the Euler method. The model (4) is solved numerically in two-dimensional space using a finite difference approximation for the spatial derivatives and an explicit Euler method for the time

integration with time steps of $\Delta t = 0.001$ and space stepsize (lattice constant) $\Delta h = 1$.

Figure 2 shows the evolution of the spatial pattern of prey in one period, with small random perturbation of the stationary solution u^* and v^* of the spatially homogeneous systems with $A = B = 1$. In this case, one can see that for the system (4), oscillatory Turing patterns emerge from the initial condition.

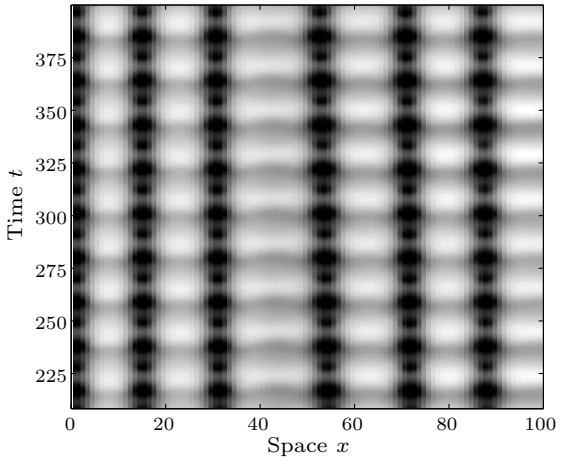

Fig. 3. Time evolution in one dimension corresponding to Fig. 2. Black means high density and white low density.

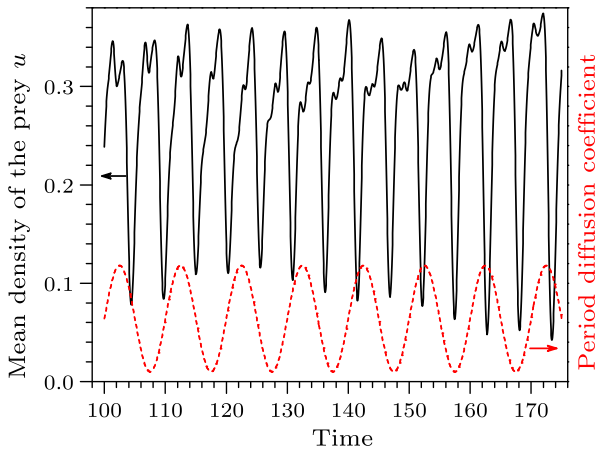

Fig. 4. The 1 : 1 frequency-locking oscillation with $A = B = 1$, and the other parameter are the same as those in Fig. 2. Upper: the mean density of the prey u. Lower: the period diffusion coefficient.

In order to see well the evolution, we show space-time plots in Fig. 3. The method of space-time plots is that let y be a constant (here, $y = 50$, the center line of each snapshots), choose the line $y = 50$, from each pattern snapshots and pile these lines in-time-order. The space-time plots show the evolution process of the prey u throughout time t and space x. From Fig. 3, we can see that there are oscillatory spatial patterns.

We find that when the amplitude A is above the threshold $A_c \approx 0.75$ (We set $\delta = 0.01$, $\gamma = 13/9$, $d_1 = 1$, $d_2 = 25$, $\eta = 0.52$, $B = 1$ and vary A. The initial value of A is zero, and the increased step of A is $\Delta A = 0.01$), the system (4) produces oscillations about period $T_{\rm out}$ with respect to the external period $T_{\rm in} = 1/B$. This phenomenon is called frequency locking (it is known that an external periodic force applied to a nonlinear pendulum can cause the pendulum to become entrained at a frequency which is rationally related to the applied frequency, a phenomenon known as frequency locking. It is useful to reveal the complexity of the ecosystem) or resonant response, i.e. when the system produces one spike within each of the M ($M = 1, 2, 3, \cdots$) periods of the external force, that is, $M : 1$ resonant response. In the present study, the output period $T_{\rm out}$ is defined as follows: T_i is the time interval between the i-th spike and the $i + 1$-th spike, q spikes are taken into account and their average value is $T_{\rm out}$, where $T_{\rm out} = \sum_{i=1}^{q} T_i/(q-1)$. Figure 4 shows that there is $1 : 1$ frequency locking in the system (4).

In summary, we have investigated the spatial pattern of a predator-prey model with a period diffusion coefficient, and obtained the oscillatory Turing pattern (cf. Fig. 2), and $1 : 1$ frequency-locking oscillation when the amplitude is above a threshold (cf. Fig. 4). Since long- and short-term temporal variations in species dispersal are frequently observed in real ecosystems, for example, in the from of seasonal and daily variations,[21] our results reveal that period dispersal may be an important mechanism for emergence of complex spatiotemporal patterns in ecosystems.

We are grateful to the anonymous referees for the meaningful suggestions.

References

[1] Tanner J T 1975 *Ecology* **56** 855
[2] Wollkind D J et al 1988 *Bull. Math. Biol.* **50** 379
[3] Saez E et al 1999 *SIAM J. Appl. Math.* **59** 1867
[4] Hassell M P 1978 *The Dynamics of Arthropod Predator-Prey Systems* (Princeton, NJ: Princeton University)
[5] Holling C S 1965 *Mem. Ent. Soc. Can.* **45** 3
[6] Peng R, Wang M and Yang G 2008 *Appl. Math. Comput.* **196** 570
[7] Hsu S B et al 1978 *SIAM J. Appl. Math.* **35** 526
[8] Hsu S U and Huang T W 1995 *SIAM J. Appl. Math.* **55** 763
[9] Levin S A, Powell T M and Steele J H 1993 *Patch Dynamics Lecture Notes in Biomathematics* (Berlin: Springer-Verlag)
[10] Hanski I and Gilpin M E 1997 *Metapopulation Biology* (San Diego: Academic)
[11] Hanski I 1999 *Metapopulation Ecology* (New York: Oxford University)
[12] Peng R and Wang M 2007 *Appl. Math. Comput.* **20** 664
[13] Peng R and Shi J 2009 *J. Diff. Equat.* **247** 866
[14] Sun G Q et al 2008 *Chin. Phys.* B **17** 3936
[15] Mukhopadhyay B and Bhattacharyya R 2006 *Bull. Math. Biol.* **68** 293
[16] Cross M C and Hohenberg P C 1993 *Rev. Mod. Phys.* **65** 851
[17] Coullet P et al 1985 *J. Phys. Lett.* **46** 787
[18] Shima S I and Kuramoto Y 2004 *Phys. Rev.* E **69** 036213
[19] Ouyang Q 2000 *Pattern Formation in a Reaction-Diffusion Systems* (Shanghai: Scientific and Technological Education Publishing House) (in Chinese)
[20] Murray JD 1993 *Mathematical Biology* 2nd edn (Berlin: Springer)
[21] Sherratt J A 1995 *J. Math. Biol.* **33** 29